Contributed Paper

Forthcoming Break-Even Conditions of Tokamak Plasma Performance for Fusion Energy Development

HIWATARI Ryoji[1)], OKANO Kunihiko[1)], ASAOKA Yoshiyuki[1)], TOKIMATSU Koji[2)], KONISHI Satoshi[3)] and OGAWA Yuichi[4)]

[1)] *Central Research Institute of Electric Power Industry (CRIEPI), Tokyo 201-8511, Japan*

[2)] *National Institute of Advanced Industrial Science and Technology (AIST), Tsukuba 305-8569, Japan*

[3)] *Institute of Advanced Energy, Kyoto University, Uji 611-0011, Japan*

[4)] *High Temperature Plasma Center, the University of Tokyo, Kashiwa 277-8568, Japan*

(Received 19 July 2005 / Accepted 12 September 2005)

The present study reveals forthcoming break-even conditions of tokamak plasma performance for the fusion energy development. The first condition is the electric break-even condition, which means that the gross electric power generation is equal to the circulating power in a power plant. This is required for fusion energy to be recognized as a suitable candidate for an alternative energy source. As for the plasma performance (normalized beta value β_N, confinement improvement factor for H-mode *HH*, the ratio of plasma density to Greenwald density fn_{GW}), the electric break-even condition requires the simultaneous achievement of $1.2 < \beta_N < 2.7$, $0.8 < HH$, and $0.3 < fn_{GW} < 1.1$ under the conditions of a maximum magnetic field on the TF coil $B_{tmax} = 16$ T, thermal efficiency $\eta_e = 30\%$, and current drive power $P_{NBI} < 200$ MW. It should be noted that the relatively moderate conditions of $\beta_N \sim 1.8$, $HH \sim 1.0$, and $fn_{GW} \sim 0.9$, which correspond to the ITER reference operation parameters, have a strong potential to achieve the electric break-even condition. The second condition is the economic break-even condition, which is required for fusion energy to be selected as an alternative energy source in the energy market. By using a long-term world energy scenario, a break-even price for introduction of fusion energy in the year 2050 is estimated to lie between 65 mill/kWh and 135 mill/kWh under the constraint of 550 ppm CO_2 concentration in the atmosphere. In the present study, this break-even price is applied to the economic break-even condition. However, because this break-even price is based on the present energy scenario including uncertainties, the economic break-even condition discussed here should not be considered the sufficient condition, but a necessary condition. Under the conditions of $B_{tmax} = 16$ T, $\eta_e = 40\%$, plant availability 60%, and a radial build with/without CS coil, the economic break-even condition requires $\beta_N \sim 5.0$ for 65 mill/kWh of lower break-even price case. Finally, the present study reveals that the demonstration of steady-state operation with $\beta_N \sim 3.0$ in the ITER project leads to the upper region of the break-even price in the present world energy scenario, which implies that it is necessary to improve the plasma performance beyond that of the ITER advanced plasma operation.

keywords:

fusion power plant, plasma performance, tokamak, break-even condition

1. Introduction

1.1 Development stages of fusion energy

Fusion energy is the origin of solar power. It can be considered the most abundant energy source in the world. Therefore, fusion energy has been estimated to be a good candidate for an alternative to fossil fuels in about 50 years. That is why it has been the subject of long-term research throughout the world.

Now, burning plasma will likely be realized soon in the International Thermonuclear Experimental Reactor (ITER) [1]. ITER is supposed to be the first device in magnetic confinement fusion systems to obtain the burning plasma, which is almost self-heated by fusion products, i.e., alpha particles. To complete the ITER project, numerous issues on plasma physics and engineering techniques have been researched. When the ITER project succeeds, fusion plasma and the reactor technology required for fusion power plants will be fundamentally demonstrated. However, it will still be difficult to clear the path to a fusion power plant from the ITER project alone.

The development strategy from ITER to a fully realized fusion power plant should be structured prudently to maximize the merits of the fusion energy and its potential contributions. In this process, the following four stages of development and their missions should be considered [2,3].

author's e-mail: hiwatari@criepi.denken.or.jp

1. **The stage for demonstration of a fusion reactor operation:** To establish plasma physics and engineering techniques for steady-state operation of burning plasma with high energy multiplication factor.
   - high efficiency of plasma current drive, reduction of heat load to the divertor plates, exhaust of helium ash, control to avoid plasma disruption.
   - steady-state plasma operation.
   - engineering techniques inevitably required for continuous energy production from a fusion reactor.
   - prospect for developing characteristics and devices inevitably required for a fusion reactor.
   - technologies for continuous tritium handling on a plant scale.
   - technologies for reliably manufacturing the large devices (superconductor coil, vacuum vessel, and so on) involved with good function as designed.
   - technologies for remote maintenance.
   - development of materials and systems against high neutron flux load.
2. **The stage for demonstration of net electric power generation as a power plant:** To establish systems and technologies inevitably required for electric power generation on a plant scale.
   - steady-state plasma operation with a high energy multiplication factor.
   - plasma performance similar to that of a commercial reactor, or a certain prospect for it.
   - flexible control method required for a commercial reactor, i.e., partial load operation, unexpected shutdown and so on.
   - an electric generation system (i.e., electric output, coolant temperature, system structure and so on) similar to that of a commercial reactor.
   - self-sustainment of tritium.
   - techniques for safety, maintenance, and waste management and disposal to advance the economic performance.
   - continuous long-term operation almost similar to that of a commercial reactor.
   - development and applicability of materials for a commercial reactor.
3. **The stage for demonstration of economic and safe performance:** To establish the safe and economical performance required for a power plant.
   - plasma performance and engineering design equal to a commercial plant.
   - specification of removable devices and systems to advance the economics of a commercial plant.
   - achievement of steady-state operation with good economy.
   - specification of merits and attraction of the fusion power plant.
4. **The stage for commercial use:** To establish the attractiveness and competitiveness of fusion energy.
   - good public acceptance promoted by stable, safe and economical operation.
   - attractive fusion power plants making the best of the advantages of fusion energy.

In the case of fast breeder reactor development, the primary development issue was the scale-up of the sodium cooling system. Hence, the thermal output had to be increased step by step. Accordingly, specific devices were built at each stage.

On the other hand, each stage in the development of the fusion power plant will not necessarily require the same type of incremental invention, because the thermal output from the experimental reactor such as ITER is inevitably large and can be gradually increased when the plasma performance improves. This implies that the experimental reactor has the potential to generate electric power similar to those of commercial reactors by replacing the blanket system with an advanced one having a higher thermal efficiency [2].

For example, the Fast Track Approach recently proposed, aiming at early realization of the fusion power plant in the 2030's, suggests a road-map somewhat different from the usual; i.e., the second and third stages mentioned above, which usually correspond to the demo and proto-type reactor stages, would be combined into a single [4,5]. On the basis of this development concept, a new development strategy is being discussed, and would be re-constructed in Japan, EU and US. While the conceptual design of SSTR was proposed as the first concept of a demonstration fusion power plant in Japan [6], recent discussion of development strategies including the Fast Track Approach has given occasion for the proposal of new concepts for a demonstration reactor such as Demo-CREST [7] and, the Fusion Demo Plant study at JAERI [8].

1.2 What are forthcoming break-even conditions ?

It is considered that there are three milestones toward the introduction of fusion energy. The first one is for the energy production to become equal to the input energy: the usual break-even condition, which has been achieved [9,10]. The second milestone is to develop plasma performance and reactor technologies so as to generate gross electric power larger than the circulating power in a power plant: i.e., the electric break-even condition. Because this milestone has not been completed, fusion energy is not currently expected as an alternative energy source even in the long-term world energy scenario. The completion of the electric break-even condition is important for fusion energy to be recognized as a suitable candidate for an alternative energy source. The third milestone is to generate electric power economically enough to be selected as the alternative energy source: that is, the economic break-even condition. When the economic break-even condition of the fusion power plant is analyzed, we have to compare the COE (cost of electricity) of the fusion power plant with that of other energy sources. Of the four stages of the previous subsection, the electric break-even condition falls between the first and second, and the economic break-even

condition falls between the third and fourth. These two break-even conditions correspond to forthcoming conditions.

1.3 How to clarify forthcoming break-even conditions ?

To clarify the electric break-even condition, the power flow analysis for a fusion power plant has to be considered. The method for this analysis is firmly established. The basic concept is summarized in Ref. [11,12]; the electric break-even condition can be systematically obtained by using a so-called "system analysis code" for fusion power plants.

On the other hand, it is impossible to predict precisely the economic break-even condition required for the introduction of fusion energy into the future world energy market, because the conditions for introducing an alternative energy source such as a fusion energy depend on the future economics of energy sources. Environmental problems and political policy may also be influences. However, we have to consider a target COE in fusion energy development, because this target of COE is required to understand the final development level of each reactor element in the fusion power plant. Hence, the economic break-even conditions discussed in the present paper should be considered as necessary conditions derived from a present-day understanding of the world energy situation; they will have to be updated accordingly. Moreover, it should be noted that the economic break-even conditions discussed here are not sufficient conditions.

Several economic analyses on fusion power plants have been carried out [13-15]. For example, Okano *et al.* carried out an economic comparison of fusion power plant with other energy sources including future innovative technologies, *e.g.*, a fast breeding reactor, a light water reactor based on uranium from sea water, a fossil fuel plant with CO_2 control, a geothermal energy plant, a wind power plant, an ocean thermal energy conversion plant, and a solar power plant, as shown in Fig. 1 [14]. This study concluded that a reasonable target

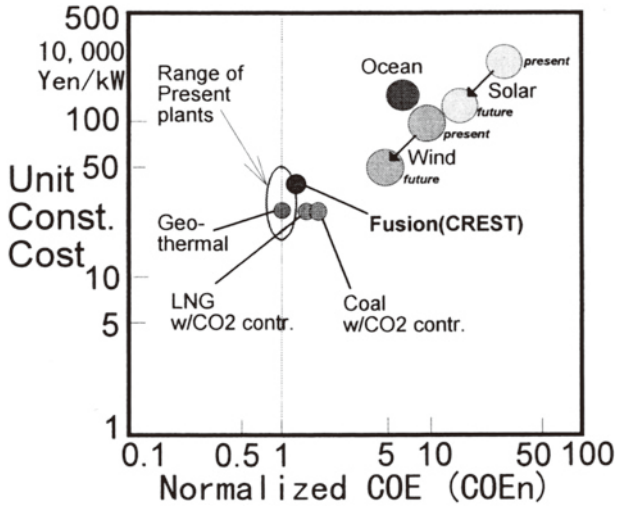

Fig. 1 Normalized COEs (COEn) and construction costs of various advanced power plants. COEn is normalized by the COE of the present-day coal plants in Japan [14].

COE for the first generation of fusion reactors should be lower than that for a CO_2-controlled fossil fuel plant, because the CO_2-controlled fossil fuel plant will be a more feasible choice from an economic view point when the COE of fusion plants exceeds that of the CO_2-controlled fossil fuel plant. Several similar economic analyses of fusion power plants have been carried; out, however, these analyses did not link the COE with the introduction year or the consequent share of fusion energy in the market.

It is important to show the required COE together with the introduction year, because it would be useless to develop a fusion power plant at a reasonable COE after another alternative energy source has been introduced as the backbone energy source. Recently, the potential of fusion energy in a long-term world energy scenario has been investigated, and the introduction year and the consequent share for the fusion energy has been estimated together with the break-even COE [16,17]. In the present study, future uncertainties, e.g. energy demand scenarios and capacity utilization ratios of options in energy/environment technologies, are considered in several different world energy scenarios. This analysis was carried out by using a long-term world energy and environmental model (this model is used for IPCC post SRES activity [18]) and estimated that the break-even price of the fusion energy for introduction in the year 2050 under the constraint of 550 ppmv CO_2 concentration (twice level at the Industrial Revolution) would be in a range from 65 mill/kWh to 135 mill/kWh (1000 mill = 1 dollar) [17]. The width of the break-even price range is derived largely from uncertainties about the future world energy scenario.

In the present study, we considered 2050 as the target year for introducing fusion energy, and we clarified the following conditions by using a fusion power plant system analysis code (FUSAC) [3]: (1) the electric break-even condition required for fusion energy to be recognized as a suitable candidate of an alternative energy source, and (2) the economic break-even condition required for fusion energy to be selected as an alternative energy source. The present study is an extension of the previous report on the electric break-even condition [19].

2. Analysis Method

2.1 Outline

The requirements for tokamak plasma performance to achieve the electric and economic break-even conditions are investigated with the database derived from the **FU**sion power plant **S**ystem **A**nalysis **C**ode (FUSAC) [3]. This system code is based on the CRIEPI cost assessment code (CCA code) [14,20], which was used to clarify β_N was the most effective parameter to reduce the COE of a tokamak reactor [14]. FUSAC consists of three main parts. The first part is a 0D plasma analysis program based on the ITER Physics Design Guidelines [21]. The second is a simple engineering design program to determine the shape of the TF coil, the position and width for the components of the tokamak reactor (blankets, shields, central solenoid coils, and bucking cylinder),

and so on. The engineering design model is based on Ref. [22]. The last part is an economic analysis program for the designed reactor based on the Generic Magnetic Fusion Reactor Model (Generomak Model) [11]. FUSAC was improved particularly for plasma and engineering design based on the CCA code.

2.2 Plasma and power flow model

The plasma parameters are calculated according to ITER Physics Design Guidelines [21], and the power flow model is basically provided with the Generomak Model [11]. An outline of calculations of plasma and power flow is illustrated in Fig. 2, and the calculation process is briefly described as follows [20].

- The main input parameters are the plasma major radius R_p, the aspect ratio A, the safety factor on plasma surface q_ψ, the average plasma temperature T_{ave}, the normalized beta value β_N, and the maximum magnetic field on TF coils B_{tmax}. The magnetic field on magnetic axis B_t is calculated here.
- The total plasma current I_p is derived from q_ψ and B_t. The total beta value β_{tot} (= β_{th} + β_α) is defined by Toroyon scaling [23], and its alpha component β_α is estimated according to Ref. [21]. The plasma volume V_p and its surface area S_p are also calculated here.
- The electron and ion densities, n_e and n_i, are derived from the beta value. The fusion power density p_f is estimated by the average plasma temperature T_{ave} and ion density n_i. The total fusion power P_f is also calculated in this step.
- The bootstrap current I_{bs} is estimated according to Ref. [21] and, consequently, the driven current I_{CD} is calculated. Confinement properties, such as the confinement improvement factor for H-mode HH, and the ratio of the Greenwald density fn_{GW} are also derived here.
- The current drive power P_{NBI}, the total thermal output P_{th}, and the averaged neutron wall load P_w^{ave} are calculated in this step. The current drive efficiency of NBI was defined by the Mikkelsen-Singer approximation [24]. The total thermal output is defined with the neutron and alpha particle components of total fusion power, P_N and P_α.

$$P_{th} = M_n f_N P_N + \eta_\alpha P_\alpha + \eta_{beam} P_{NBI} , \qquad (1)$$

where M_n, f_N, η_α, and η_{beam} are the multiplication factor of neutron energy in the blankets, the covering fraction of the blanket for the plasma surface, the collecting rate for the energy of alpha particle, and the collecting rate for the NBI input power, respectively. In this study, f_N = 0.9, η_α = 0.7, and η_{beam} = 0.7 are assumed. It is necessary to design the blanket so as to fix the multiplication factor of neutron energy in the blankets; however, details of the blankets are uncertain at present. Hence, the conservative value M_n = 1.1 is assumed in the present study in consideration of the use of solid breeders, Li_2O, Li_2TiO_3, or Li_2ZrO_3, with 100% density at room temperature [25].

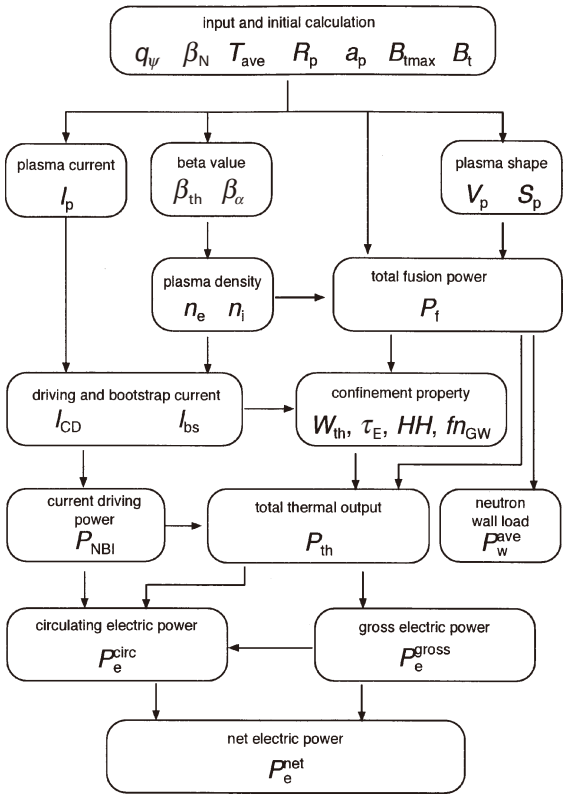

Fig. 2 Calculation flow for plasma performance and power flow in FUSAC.

- The circulating power P_e^{circ} is estimated by the Generomak Model [11], and the gross electric power P_e^{gross} is also calculated in this step.
- Finally, the net electric power P_e^{net} is obtained.

Physical and engineering parameters are defined in Ref. [21] and Ref. [11], respectively.

This 0D model for plasma property has produced satisfactory results in the ITER design and other reactor designs, when one roughly estimates the operational region for plasma parameters of a tokamak reactor as seen in Ref. [26]. The parameter ranges of the 0D system analysis are listed in Table 1. The maximum major radius is restricted to 8.5 m, similar to that of ITER-FDR [27], because of the machine construction cost. The ranges for aspect ratio, plasma elongation, plasma triangularity, plasma temperature, and surface safety factor were selected based on experimental data and past reactor designs.

Of course, the 0D model cannot precisely take several effects into account, such as a realistic heating/current drive profile, line radiation loss power localized in the edge region, bootstrap current fraction, advanced operation with negative shear and so on. When the operation point of a reactor design is selected, a detailed analysis of plasma performance will be additionally required with specialized analysis code for MHD, transport, and current drive properties. Moreover, the optimization of a design parameter set is not sufficient

Table 1 The parameter ranges 0D system analysis.

Major radius R_p (m)	5.5~8.5
Aspect ratio A	3.0~4.0
Plasma elongation κ	1.5~2.0
Plasma triangularity δ	0.35~0.45
Plasma temperature T_{ave} (keV)	12~20
Plasma surface safety factor q_ψ	3.0~6.0
Max. magnetic field B_{tmax} (T)	13, 16, 19
Thermal efficiency η_e (%)	30, 40
NBI system efficiency η_{NBI} (%)	30, 50, 70

in this parametric analysis. For example, it is necessary to increase the plasma elongation so as to get the clear merit of a low aspect ratio smaller than 3.0 [28]; however, the constant elongation in all aspect ratios in Table 1 is applied to this parametric analysis. Therefore, the results discussed in the present paper mainly focuse on the conventional tokamak region ($3 \le A \le 4$) in Table 1.

2.3 Guidelines for reactor technology

The demonstration plant for the realization of net electric power generation has to be designed with reasonably foreseeable conditions. In this study, the following engineering parameters are considered as references: thermal efficiency of electric conversion η_e = 30%, NBI system efficiency η_{NBI} = 50%, and magnetic field on TF coils B_{tmax} = 16 T. These reference parameters are based on the present development status and the ITER test blanket module plan. The maximum magnetic field of TF coils B_{tmax} = 13 T with Nb_3Al [29] and the NBI system efficiency η_{NBI} = 30 ~ 40% [1] are applicable to ITER. The thermal efficiency of electric conversion is assumed to be almost the same as that of a typical light water reactor, because the coolant conditions on the test breeding blanket proposed in the ITER program are similar to those of a typical light water reactor [30].

In addition to these parameters, three other conditions are considered in the present study. First, the current drive power P_{NBI} is limited to 200 MW, because of the limit of available NBI ports and the necessity of having a small circulating power. In the ITER NBI design, the injection power for a port is 16.5 MW [1]. If an injection power of 33.0 MW, twice the ITER design value, becomes possible, the total NBI power of 200 MW requires 6 ports, which is considered the maximum port number in the present paper. Of course, the NBI power should be as small as possible, but P_{NBI} ~ 200 MW is required to sustain the plasma current for conservative plasma performance. Second, a sufficient space of 1.4 m for the blankets and shields is maintained, because a tritium breeding ratio larger than 1.0 (TBR ≥ 1.0) has to be securely achieved. Finally, the plasma current ramp-up is provided with the magnetic flux swing of the CS coils. The required magnetic flux Ψ_{ramp} is defined as follows:

$$\Psi_{ramp} = \left(L_p + \mu_0 C_{Ejima} R_p\right) I_p , \tag{2}$$

where L_p, R_p, and I_p are, respectively, the plasma inductance, the plasma major radius, and the plasma current with the Ejima coefficient C_{Ejima}(= 0.45) and permeability of vacuum μ_0 [26].

These engineering constraints are not absolute, but will depend on the development of engineering elements and plasma operation techniques in the future. When more advanced parameters are firmly established in the ITER program, such advanced parameters should, of course, be applied. The sensitivity analysis for these engineering conditions is discussed in Sec. **3.3**.

2.4 Database for plasma operational points

With extensive analyses by using the fusion power plant system analysis code (FUSAC), a database for about 100,000 operational points has been constructed with the conditions mentioned in the previous subsection. Those data cover the plasma parameter ranges listed in Table 1. With this database, investigation of the plasma performance was carried out. The main elements of the database are plasma performance parameters (β_N, HH, fn_{GW}), plasma configuration parameters (major radius R_p, aspect ratio A, plasma elongation κ, plasma triangularity δ), other plasma parameters (temperature T_{ave}, plasma densities n_e, n_i, plasma current I_p, bootstrap current I_{bs} and so on), and engineering parameters (coil shape and its location, flux supply with CS coils Ψ_{CS}, net electric power P_e^{net}, circulating power P_e^{circ} and so on).

The database also contains economic parameters, such as the cost of electricity and the construction cost. These elements will be applied to the analysis of the economic break-even condition in Sec. **4**.

3. Electric Break-even Condition for Practical Energy Source

3.1 The plasma performance required for net electric power and its characteristics

The normalized beta value (β_N), the confinement improvement factor for H-mode scaling (HH), and the ratio of Greenwald density limit (fn_{GW}) are considered the representative parameters for plasma performance. These parameters are defined as follows:

$$\beta_N = \beta_{tot} \Big/ \left(\frac{I_p}{a_p B_t}\right), \tag{3}$$

$$HH = \tau_E \Big/ \tau_{E,th}^{IPB98(y,2)}, \tag{4}$$

$$fn_{GW} = n_e \Big/ n_{GW} , \tag{5}$$

where I_p, a_p, B_t, and n_e are the total plasma current, the plasma minor radius, the toroidal magnetic field on the magnetic axis, and the averaged electron density, respectively. The scaling law of energy confinement time for H-mode $\tau_{E,th}^{IPB98(y,2)}$ is defined as [31]

$$\tau_{E,th}^{IPB98(y,2)} = 0.0562 I_p^{0.93} B_t^{0.15} P^{-0.69} \times \bar{n}_{19}^{0.41} M^{0.19} R_p^{1.97} \varepsilon^{0.58} \kappa^{0.78}, \quad (6)$$

where P, $\bar{n}_{19}$, R_p, M, ε, and κ are the loss power (MW), the line average density (10^{19} m^{-3}) the plasma major radius (m), the fuel mass number (amu), the inverse aspect ratio, and the plasma elongation, respectively. The definition of the Greenwald density is [32]

$$n_{GW} = I_p \Big/ \left(\pi a_p^2\right). \quad (7)$$

The requirements for a tokamak reactor to generate net electric power were investigated for these plasma performance parameters.

The plasma performance parameters β_N, HH, and fn_{GW} required for P_e^{net} = 0, 400 and 1000 MW are plotted in Figs. 3. These results assume B_{tmax} = 16 T, η_{NBI} = 50%, η_e = 30%, $P_{NBI} \leq$ 200 MW, κ=1.9 and δ = 0.45. The electric break-even (P_e^{net} = 0 MW) condition for normalized beta has a range of $1.2 \leq \beta_N \leq 2.7$ as shown in Fig. 3(a1). The width of β_N plots for each net electric power derives mainly from the major radius; that is, the plots for β_N = 1.2 and β_N = 2.7 in the case of P_e^{net} = 0 MW correspond to R_p = 8.5 m and R_p = 6.0 m, respectively. For P_e^{net} ~ 1000 MW, $\beta_N \geq 3.0$ is required.

In the present paper, the NBI power is restricted to 200 MW. When this restriction is changed, the requirement for a tokamak reactor to generate net electric power will be also changed. The dependence of the P_{NBI} restriction on the β_N requirement for P_e^{net} = 1000 MW is shown in Fig. 3(a2). As the restriction of NBI power increases from $P_{NBI} \leq$ 100 MW to $P_{NBI} \leq$ 300 MW, the lower limit of operational region of β_N is reduced from β_N ~ 3.5 to β_N ~ 2.8. P_{NBI} ~ 300 MW may become practical in the future, but the following results are provided under the condition of $P_{NBI} \leq$ 200 MW, because of the engineering consideration of the NBI port number discussed in Sec. **2.3**.

Regardless of the net electric power P_e^{net}, it should be noted in Fig. 3(b1) that at least $HH \geq 0.8$ is required for net electric power generation with the restriction of $P_{NBI} \leq$ 200 MW. The operational range of P_e^{net} = 1000 MW apparently shrinks in the region of $HH \geq 1.5$ in comparison with that of P_e^{net} = 0, 400 MW, because the HH operating points of P_e^{net} = 1000 MW with $HH \geq 1.5$, which have a large β_p and a small plasma current, result in a larger bootstrap current than the total plasma current. Therefore, such operating points with a bootstrap current fraction greater than one are excluded in the present paper. When an advanced plasma is considered for a reactor design, *e.g.* as discussed in the CREST (β_N ~ 5.0 and f_{bs} ~ 0.8) [33], the application of the present result should be carefully made, because the 0D plasma model used in the present paper cannot precisely deal with an advanced operation with negative magnetic shear. The operational region of HH also depends on the P_{NBI} restriction. The effect of the P_{NBI} restriction on the HH required for P_e^{net} = 1000 MW is shown in Fig. 3(b2). According to this figure, the larger

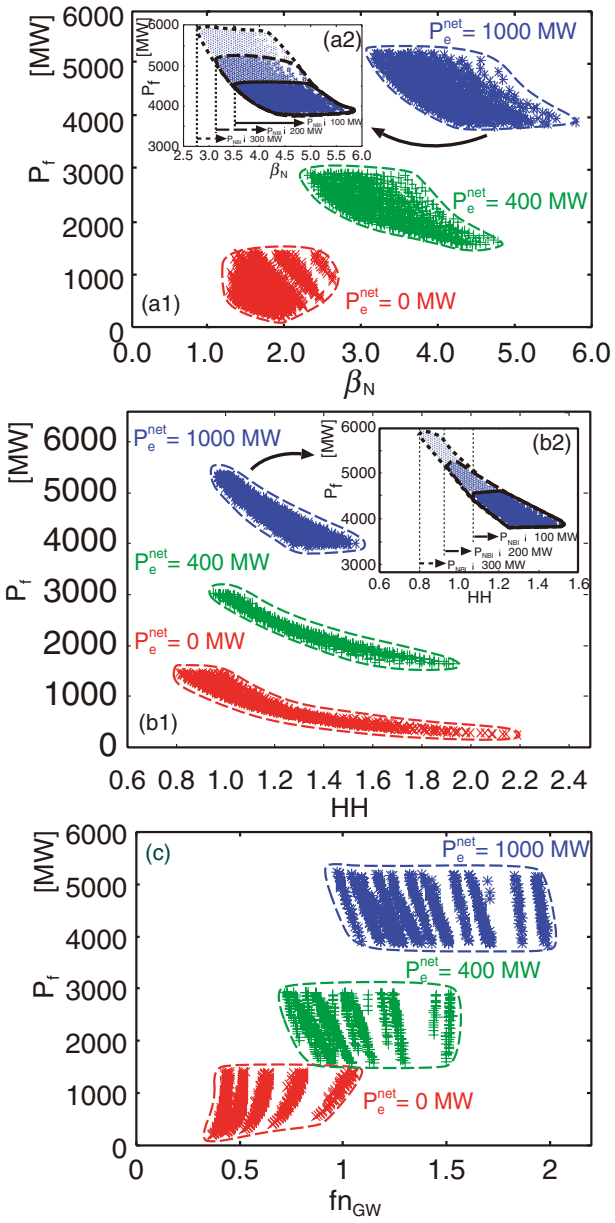

Fig. 3 Plasma performance required for each net electric power P_e^{net} = 0, 400, 1000 MW. The upper band edge is for R_p = 6.0 m while the lower band edge is for R_p = 8.5 m. (a1) the required β_N for each net electric power, (a2) the dependence on P_{NBI} restriction of the required β_N for P_e^{net} = 1000 MW, (b1) the required HH for each net electric power, (b2) the dependence of P_{NBI} restriction on the required HH for P_e^{net} = 1000 MW, (c) the required fn_{GW} for each net electric power.

the restriction of P_{NBI}, the lower the limit of the operational region for HH.

A large fn_{GW} is required as P_e^{net} becomes large as shown in Fig. 3(c); this tendency is similar to that of β_N. The electric break-even (P_e^{net} = 0) condition is provided with the fraction of Greenwald density within the range of $0.3 \leq fn_{GW} \leq 1.1$. When P_e^{net} = 1000 MW is the target, at least $fn_{GW} \geq 0.9$ is required. The restriction of P_{NBI} also affects the operational region of fn_{GW} as shown in Figs. 3(a2) and (b2), but the effect is not seen so clearly for fn_{GW}.

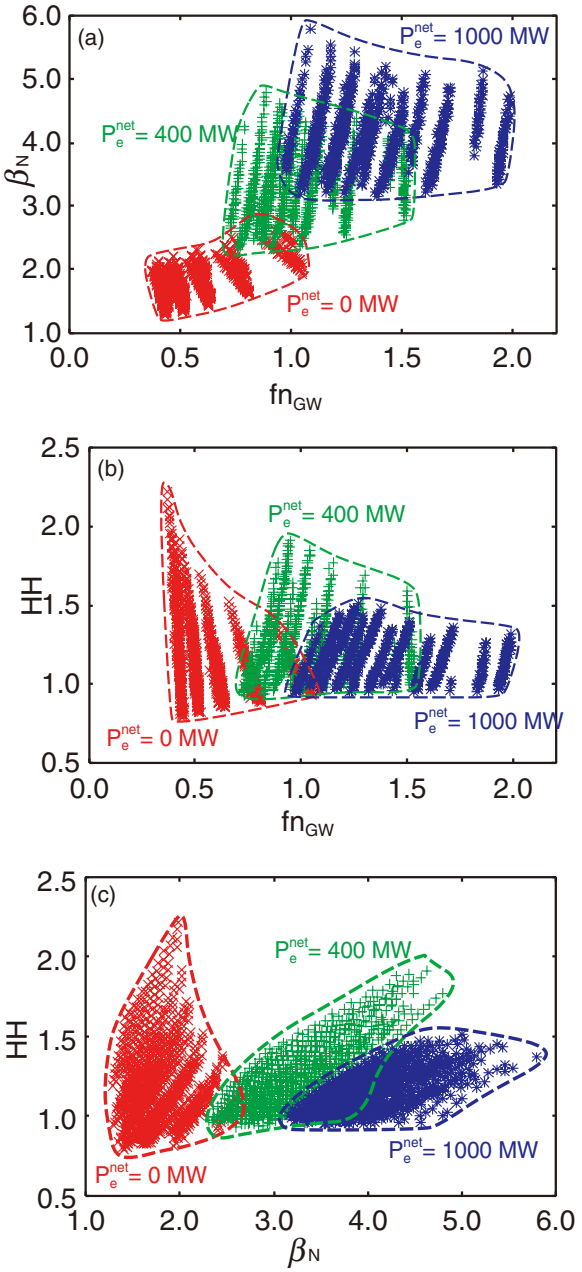

Fig. 4 The relationship between plasma performance parameters required for P_e^{net} = 0, 400, 1000 MW. The upper band edge is for R_p = 6.0 m while the lower band edge is for R_p = 8.5 m. (a) the relationship between β_N and fn_{GW}, (b) the relationship between fn_{GW} and HH, (c) the relationship between HH and β_N.

The relationships among plasma performance parameters, β_N, HH, and fn_{GW} are shown in Fig. 4. As shown in Fig. 4(a), β_N and fn_{GW} have to be increased together in order to increase net electric power. However, in Figs. 4(b) and 4(c), clear relationship does not emerge between HH and the other parameters, such as β_N and fn_{GW}, though, it should be noted that there is no operational point in the range of $HH \leq 0.8$. Therefore, the accomplishment of $HH \sim 1.0$ is inevitable for realizing net electric power from a fusion power plant, under the condition of $P_{NBI} \leq 200$ MW.

According to Figs. 3 and 4, increases in both β_N and fn_{GW}

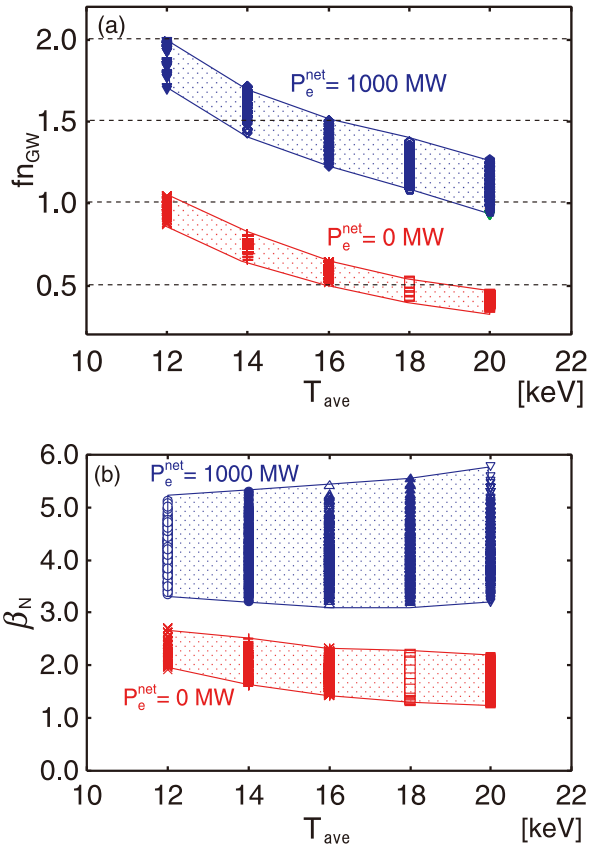

Fig. 5 The effect of average plasma temperature T_{ave} on (a) fn_{GW} and (b) β_N for each net electric power P_e^{net} = 0, 1000 MW. The upper band edge is for R_p = 6.0 m while the lower band edge is for R_p = 8.5 m.

are inevitably required to increase the net electric power, but HH does not have this tendency. Consequently, the net electric power P_e^{net} = 0 MW requires the simultaneous achievement of $1.2 \leq \beta_N$ 2.7, $0.8 \leq HH$ and $0.4 \leq fn_{GW} \leq 1.1$, under the engineering conditions mentioned in Sec. **2.3**. It should be noted that the relatively moderate plasma performance of β_N = 1.8, HH = 1.0 and fn_{GW} = 0.85, which corresponds to the ITER reference plasma performance for inductive operational scenario, can realize P_e^{net} = 0 MW and has the potential to obtain P_e^{net} < 400 MW with $R_p \leq 8.5$ m. When P_e^{net} = 1000 MW is the target, simultaneous achievement of $\beta_N \geq 3.0$, $HH \geq 1.0$ and $fn_{GW} \geq 1.0$ is required.

The plasma temperature T_{ave} has an effect on the required plasma performance parameters, especially on fn_{GW} as shown in Fig. 5, because the plasma density decreases when plasma temperature increases at a constant fusion power. In Fig. 5(a), fn_{GW} required for P_e^{net} = 0 MW and 1000 MW decreases with increasing plasma temperature. On the other hand, in Fig. 5(b), the normalized beta value required for net electric power does not have a clear dependence on the plasma temperature. As a result, higher plasma temperature is the key to relieving fn_{GW} requirements at constant fusion power. The upper limit of the plasma temperature depends on the divertor conditions from an engineering point of view, because increasing plasma temperature results in excessive heat load on the divertor

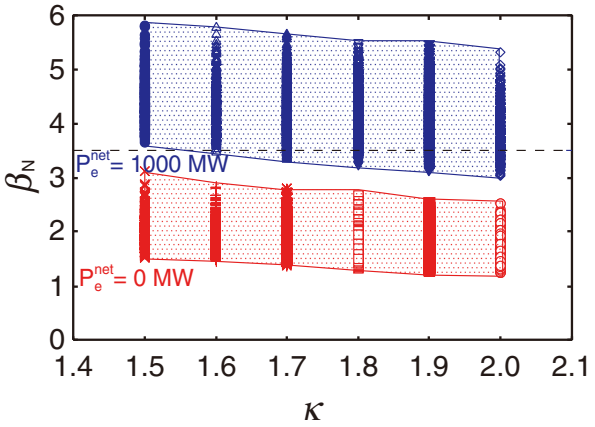

Fig. 6 The dependence of κ on the required β_N for each net electric power P_e^{net} = 0, 1000 MW. The upper band edge is for R_p = 6.0 m while the lower band edge is for R_p = 8.5 m.

plates. A careful investigation of divertor conditions is needed to select the upper limit of the plasma temperature. When a plasma temperature T_{ave} ~ 20 keV is permitted, the electric break-even condition is easy to achieve with $fn_{GW} < 0.5$, and P_e^{net} = 1000 MW is also attainable with fn_{GW} ~ 1.0. Generally, β_N can be reduced by either increasing plasma elongation or the toroidal magnetic field. The effect of plasma elongation on β_N is shown in Fig. 6. An increase from κ = 1.5 to κ = 2.0 results in reducing β_N by about 0.5 for both the P_e^{net} = 0 MW and P_e^{net} = 1000 MW cases. In the system code used here, the plasma beta value is defined by $\beta = \beta_N I_p/(a_p B_t)$, and a decrease in the required β_N is caused by the increase of plasma current I_p, because of the increase in plasma elongation with a constant surface plasma safety factor. When P_e^{net} = 1000 MW is desired, $\beta_N \geq 3.5$, which is larger than the ideal MHD beta limit [23], is required for the κ = 1.5 case. On the other hand, κ = 2.0 has the potential to obtain P_e^{net} = 1000 MW with $\beta_N \leq 3.5$. From these results, $\kappa \geq 2.0$, which has been considered in the recent design studies of commercial reactors such as CREST [33] and ARIES-AT [34], is confirmed as a reasonable goal for tokamak fusion plants. This issue has, however, a very important relationship with the engineering design, i.e., blanket and shield design, control coil location, and so on, because of the positional instability. Accordingly, careful consideration is required when a plasma elongation κ ~ 2.0 is selected in a reactor design. It should be noted that the aspect ratio of $3 \leq A \leq 4$ is assumed in the present paper, and the upper limitation of κ is generally moderated in the region of a low aspect ratio.

3.2 Plasma performance diagram on Q vs. P_f (energy multiplication factor and fusion power) space

In the previous subsection, the various conditions for a tokamak reactor to demonstrate net electric power are investigated under engineering conditions. When the first tokamak reactor to demonstrate net electric generation is designed, these results should be taken into consideration. At that time,

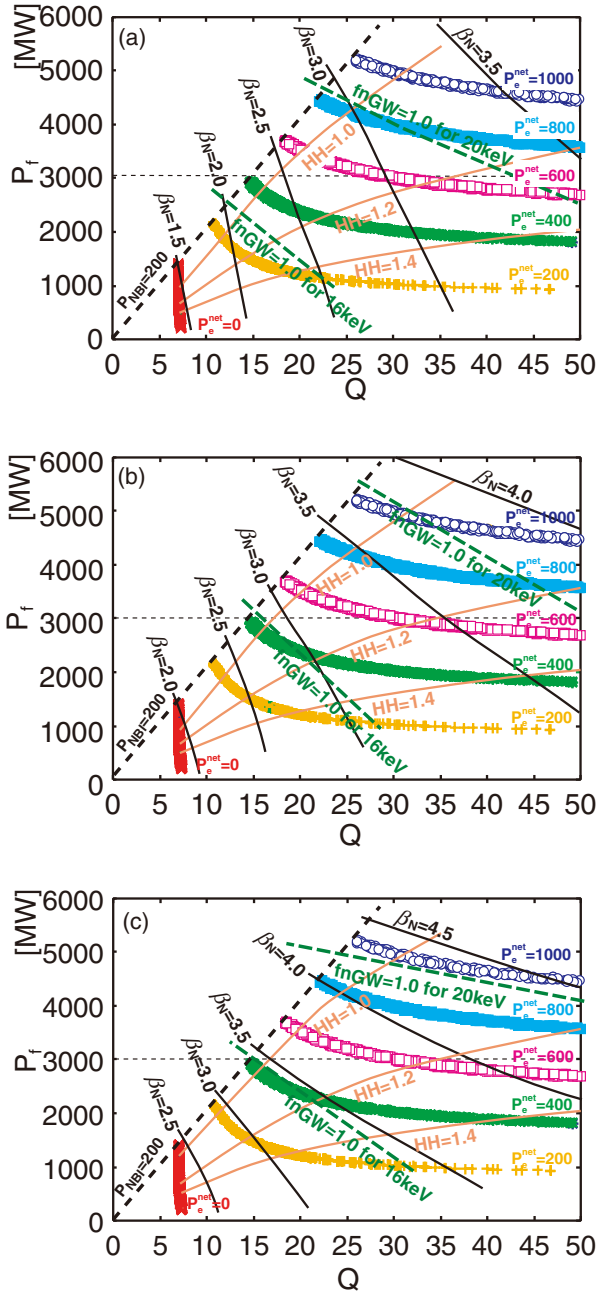

Fig. 7 Plasma performance diagram on Q vs. P_f space for (a) R_p = 8.5 m, (b) R_p = 7.5 m, (c) R_p = 6.5 m. Each line of β_N, HH, and fn_{GW} delineate the respective attainable boundary. The fn_{GW} boundary has two lines for plasma operation temperature T_{ave} = 16 keV and 20 keV.

one of the initial tasks will be to select the plasma major radius which has a sufficient capacity to produce the target fusion power. Therefore, it is essential to comprehend the relationship between the requirement of plasma performance for a given fusion power and the major radius.

Figures 7 describe the attainable region with several plasma performances of β_N, HH, and fn_{GW}, on Q vs. P_f (energy multiplication factor and fusion power) space for each major radius R_p of 8.5 m, 7.5 m, and 6.5 m. These figures are depicted under the engineering conditions of $P_{NBI} \leq 200$ MW, η_e = 30%, η_{NBI} = 50%, and B_{tmax} = 16 T. Each figure consists

of two plots. One is the plot for net electric power P_e^{net} on Q vs. P_f; the other is for plasma performance parameters on Q vs. P_f. The former relationship is evident for the given engineering parameters. The latter is derived in the previous subsection. Simply speaking, Fig. 7 comprise superpositions of the above two plots. With these figures, a brief estimation of the plasma performance required for a tokamak reactor to generate net electric power can be made. The plasma performance lines for β_N, HH, and fn_{GW} in Fig. 7 delineate the attainable boundaries of the respective plasma performance. For example, $fn_{GW} > 1.0$ is always needed for the domain above the line of $fn_{GW} = 1.0$, but not for the domain below line. It should be noted that the domain below the line of $fn_{GW} = 1.0$, where all the operational points of $fn_{GW} \leq 1.0$ are contained, also includes operational points with $fn_{GW} \geq 1.0$. Similarly, the other plasma parameter lines shown in Fig. 7 delineate respective attainable boundaries. In these figures, the operational points for each net electric power only with $P_{NBI} \leq 200$ MW are plotted for the engineering conditions discussed in Sec. **2.3**.

The attainable region with $R_p = 8.5$ m is depicted on Q vs. P_f space in Fig. 7(a). This figure shows that a moderate normalized beta value of $\beta_N \sim 1.5$ has the potential to achieve $P_e^{net} = 0$ MW with $HH \sim 1.0$ and $fn_{GW} \leq 1.0$. When $P_e^{net} = 600$ MW, which corresponds to $P_f \sim 3000$ MW with $\eta_e = 30\%$, is the target with $R_p = 8.5$ m, the required β_N becomes about $\beta_N \sim 3.0$. In Fig. 7, two attainable boundaries of fn_{GW} are delineated for plasma temperatures of $T_{ave} = 16$ keV and $T_{ave} = 20$ keV. In the case of $R_p = 8.5$ m, the condition of Greenwald density is more severe than in case of smaller major radius. Specifically, an electric power larger than $P_e^{net} = 200$ MW cannot be attained with $fn_{GW} < 1.0$ under the condition of $T_{ave} \leq 16$ keV. Furthermore, it should be noted that the construction cost for $R_p = 8.5$ m is relatively high.

According to Fig. 7(b), the requirement for β_N to achieve $P_e^{net} \sim 0$ MW with $R_p = 7.5$ m becomes fairly demanding, i.e., $\beta_N \sim 2.0$. This figure shows that the progress of the ITER program as planned at present will enable achieving electric break-even ($P_e^{net} = 0$ MW) with a major radius $R_p = 7.5$ m. In addition, Fig. 7(b) shows that it is possible to attain $P_e^{net} \sim 600$ MW with $P_f \sim 3000$ MW using $\beta_N \leq 3.5$, which is considered to be the ideal MHD beta limit. This plasma performance of $\beta_N \sim 3.5$ can be examined with ITER.

In case of the $R_p = 6.5$ m in Fig. 7(c), the β_N requirement for $P_e^{net} = 0$ MW with $R_p = 6.5$ is about $\beta_N \sim 2.5$, which is larger than that of the ITER reference parameter. When $P_f \sim 3{,}000$ MW is the target with $R_p = 6.5$ m, it is necessary to attain $\beta_N > 3.5$, which may require some stabilizing effects, *e.g.* using a conducting wall in the blanket. However, if it is possible, its construction cost is considered to be moderate and the perspective for demonstrating its economic performance is relatively easy to obtain.

According to the comparison of Fig. 7, β_N depends on the major radius R_p. The dependence of the required β_N on R_p corresponds to the width of operational plots for β_N in Fig. 3(a1). On the other hand, the attainable boundary of HH is almost parallel to the restriction of P_{NBI}, which means that the restriction of P_{NBI} has a great impact on HH. Moreover, Fig. 7 reveal that improvement in HH at a constant β_N cannot always increase the net electric power. It is also found in Fig. 7 that the fn_{GW} requirement depends on the plasma temperature. $P_f \geq 3{,}000$ MW cannot be attained with $fn_{GW} < 1.0$ under the condition of $T_{ave} \leq 16$ keV.

Taking the above results into account, we found that the major radius $R_p \sim 7.5$ m may be reasonable for early realization of a demonstration plant, as mentioned in Sec. **1**, because both of the electric break-even condition ($\beta_N \sim 1.8$, $HH \sim 1.0$, $fn_{GW} \sim 0.9$) and $P_e^{net} \sim 600$ MW condition ($\beta_N \sim 3.5$, $HH \sim 1.2$, $fn_{GW} \sim 1.0$) can likely be investigated within the ITER program parameters [1]. This major radius is similar to that of SSTR [6], and it also corresponds to the design point of Demo-CREST [7]. Furthermore, $P_e^{net} \sim 1000$ MW with $R_p = 7.5$ m, under the conditions of $\beta_N \sim 3.5$, $HH \sim 1.2$, and $fn_{GW} \sim 1.0$, may become possible by replacing the blanket of $\eta_e = 30\%$ with an advanced one of $\eta_e \geq 40\%$. In other words, the perspective of economic performance may be examined with a single device of $R_p = 7.5$ m.

Of course, the choice of the major radius for a demonstration reactor depends on the basic policy of the reactor design. In the present paper, we adopted the conservative engineering conditions mentioned in Sec. **2.3**. Hence, a different policy from ours may lead to a different optimization as for the major radius.

3.3 Consideration

3.3.1 About the reference engineering conditions

The demonstration plant should not be always limited to conservative engineering conditions, *e.g.*, $\eta_e \sim 30\%$, $\eta_{NBI} \leq 50\%$, and $B_{tmax} \leq 16$ T, if one assumes the development of sufficient engineering technologies in addition to that of advanced plasma. However, it is also necessary for the demonstration plant design to select actually foreseeable engineering conditions, since early construction of a demonstration plant just after or during the ITER program is being seriously considered, as the fast track approach [5]. That is why we emphasize conservative engineering conditions in the present paper. At the same time, it is essential for attractive fusion power plants in the future to improve the engineering conditions, such as a high thermal efficiency $\eta_e \geq 40\%$ as proposed in the commercial plant concept of CREST [33]. In this section, the effects of engineering conditions are investigated and their contributions to mitigating the plasma performance required for net electric generation is discussed.

3.3.2 The effect of thermal efficiency

Improvement in thermal efficiency for electric power plants is preferable for achieving net electric power generation. This issue is applicable not only to fusion power plants but also to other electric power plants. It is easy to show that improvement in thermal efficiency mitigates the plasma performance conditions required for a certain net electric power. In the case of a thermal efficiency $\eta_e = 40\%$, the attainable boundaries of each plasma performance on Q vs. P_f space

are delineated in Fig. 8, under the same conditions as in Fig. 7(b). The attainable boundaries of β_N and *HH* in Fig. 8 are almost the same as those in Fig. 7(b). In comparison with Fig. 7(b), the plots of each net electric power for $\eta_e = 40\%$ can be realized with a smaller fusion power than that for $\eta_e = 30\%$. Basically, the difference between Fig. 8 and Fig. 7(b) lies in the plots of each net electric power.

The electric break-even ($P_e^{net} = 0$ MW) condition for $\eta_e = 40\%$ is attainable with $\beta_N \sim 1.5$ and $HH \sim 1.0$, which is less demanding than that planned for the ITER operation scenario. Therefore, when $\eta_e = 40\%$ is achieved, it will become possible to design a demonstration plant with a major radius $R_p \leq 7.5$ m. On the other hand, the net electric power of $P_e^{net} \sim 900$ MW with $\eta_e = 40\%$, which corresponds to a fusion power $P_f = 3000$ MW with $Q = 35$, is attainable with $\beta_N \sim 3.5$ and $HH \sim 1.2$. In comparison with the case of $\eta_e = 30\%$ of Fig. 7(b), the net electric power increases from 600 MW to 900 MW. This implies that the first demonstration plant with $R_p = 7.5$ m and $\eta_e = 30\%$ holds the promise of potentially generating a net electric power of $P_e^{net} = 900$ MW with $\beta_N \leq 3.5$ and $HH \leq 1.2$ by replacing the blanket. Such upgrading capability is one of the merits of fusion reactors and should be noted when the development strategy of fusion energy is discussed.

3.3.3 The effect of NBI system efficiency

It is also important for a fusion reactor to improve the NBI system efficiency for small circulating power. At present, the NBI system efficiency of $\eta_{NBI} = 30 \sim 40\%$ is supposed to be achievable, if the ITER program is implemented as planned [1]. The attainable boundaries of each plasma performance with the same conditions as in Fig. 7(b), except $\eta_{NBI} = 30\%$, are shown on Q vs. P_f space in Fig. 9. The attainable boundary of each plasma performance is roughly similar to that in Fig. 7(b). The operational plots of each net electric power for a high Q value near $Q \sim 50$ in Fig. 9 are almost the same as those in Fig. 7(b). On the other hand, as the Q value decreases, the required fusion power for each net electric power increases more than that of the $\eta_{NBI} = 50\%$ case in Fig. 7(b), which results in an increase of the β_N required for each net electric power. The electric break-even condition can not be attained with $\beta_N < 2.0$, as described in Fig. 9. In other words, improvement in η_{NBI} to mitigate the β_N required for net electric power is more important for a low-Q reactor than for a high Q reactor. Therefore, a high-efficiency NBI system should be developed for construction of a demonstration plant with a small Q. Of course, the NBI system efficiency η_{NBI} has an effect on the construction cost of a fusion power plant, and improvement in NBI system efficiency is also important for a commercial reactor with a high Q value.

3.3.4 Selection of high magnetic field

Selection of a high magnetic field in reactor design is one of the reasonable ways to improve economic performance as seen in the design concept of A-SSTR2 [35]. The effect of increasing B_{tmax} from 13 T to 19 T on the normalized beta value β_N for respective P_e^{net} is shown in Fig. 10. In the case of $B_{tmax} = 13$ T, the operational region of $P_e^{net} = 0$ MW for $\beta_N \leq 1.8$, which corresponds to the ITER reference parameter, is

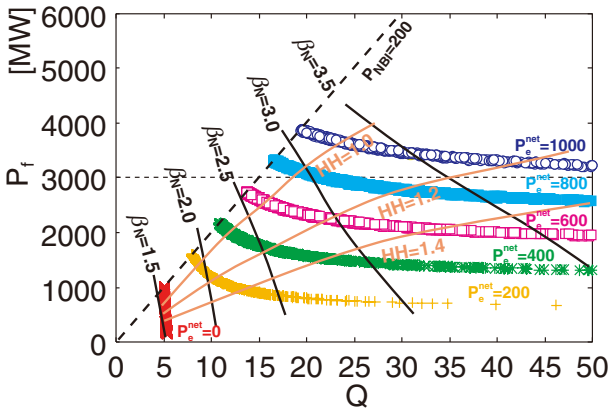

Fig. 8 Plasma performance diagram on Q vs. P_f space for R_p = 7.5 m with the same conditions as Fig. 7(b) except thermal efficiency η_e = 40%.

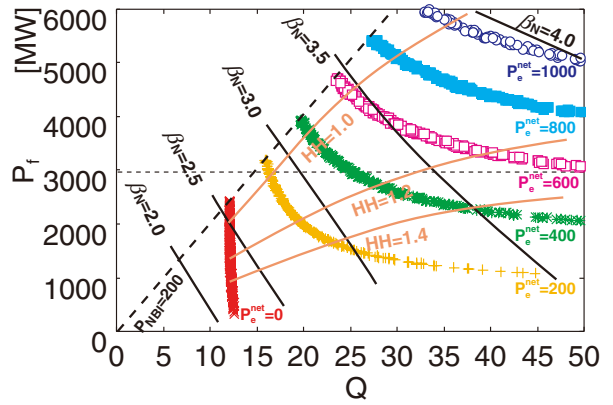

Fig. 9 Plasma performance diagram on Q vs. P_f space for R_p = 7.5 m with the same conditions as Fig. 7(b) except NBI system efficiency η_{NBI} = 30%.

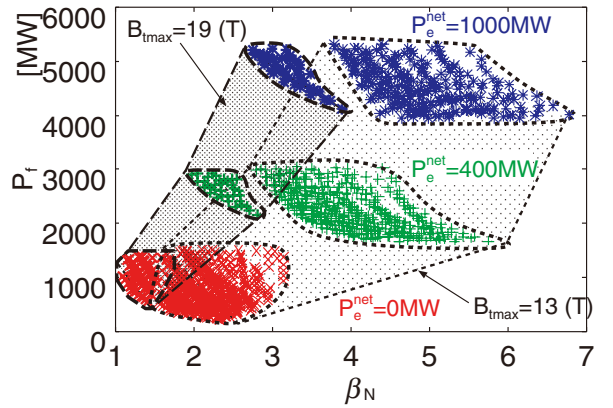

Fig. 10 The effect of B_{tmax} on the required β_N for each net electric power P_e^{net} = 0, 400, and 1,000 MW. The upper band edge is for R_p = 6.0 m while the lower band edge is for R_p = 8.5 m.

narrow. Altogether, a reactor design with $B_{tmax} = 13$ T and $\beta_N \sim 1.8$ requires a relatively large major radius $R_p \geq 8.0$ m for net electric power; such a large reactor size seems unattractive in terms of its economic performance as an electric power

plant. In addition, the operational region of P_e^{net} = 1000 MW is not achievable under the condition of the ideal MHD beta limit, $\beta_N \leq 3.5$.

With the increase of B_{tmax} from 13 T to 19 T, the minimum value for β_N is reduced by about 1.0. While the operational regions for P_e^{net} = 0, 400, and 1000 MW shrink in the part of large β_N. In the present study, a bucking cylinder and CS coils are located within the central torus region and an additional torus space of 1.4 m is kept to accommodate blanket and shield installation. The reason for the shrinking operational region in the case of B_{tmax} = 19 T is that magnetic stress on TF, CS, and the bucking cylinder becomes too large to ensure the torus space for these structures with a major radius $R_p \leq 7.5$. Consequently, the operation region for each P_e^{net} for B_{tmax} = 19 T becomes narrow in comparison with the case of B_{tmax} = 13 T. Therefore, the selection of a high magnetic field requires a sophisticated radial build adopting advanced techniques in the central torus region. For example, if the technique of current ramp-up without CS coils, which was recently investigated in JT-60U [36], is firmly established in the ITER program, a reactor with high magnetic field such as $B_{tmax} \sim 20$ T may become a practical candidate for a demonstration plant and a commercial plant.

3.3.5 The condition of blanket design

The averaged neutron wall loads P_w^{ave} for P_e^{net} = 0, 400, and 1000 MW are shown in Fig. 11. This figure is under the same conditions as in Figs. 3. The width of each P_e^{net} is mainly caused by the plasma major radius. The minimum plot of P_w^{ave} in each P_e^{net} corresponds to the plasma major radius of $R_p \sim 8.5$ m. Similarly, the maximum values correspond to $R_p \sim 6.0$ m. This figure implies requirements for the materials of the first wall and the tritium breeding ratio (TBR). When $P_f \sim$ 3,000 MW is the target, material for the first wall sustaining an average neutron wall load 1.0 MW/m^2 $\leq P_w^{ave} \leq$ 3.5 MW/m^2 is required. TBR $\geq$ 1.0, which has to be surely demonstrated in the demonstration plant after ITER, is essential for a fusion power plant. This figure also implies the design condition of the neutron wall load for the breeding blanket for each net electric power level.

According to this figure, when a demonstration plant with P_f = 3000 MW and R_p = 7.5 m proposed in Sec. **2.3** are the target, P_w^{ave} should be about 2.0 MW/m^2. This $P_w^{ave} \sim 2.0$ MW/m^2 is not as severe as $P_w^{ave} \sim 4.5$ MW/m^2 seen in CREST [33], both for the materials of the first wall and for TBR.

4. Economic Break-even Condition as a Necessary Condition

4.1 Economic analysis model for fusion power plant

In the present study, the costs of all elemental devices in a fusion plant are calculated by multiplying a unit cost per weight constant. This calculation method is widely admitted and used in cost studies. It is considered that the cost will depend largely on the volume or weight of components at the time when the required processing techniques for building fusion components have matured. Costs of all the other equipment are calculated by nonlinear scaling to a standard cost value either by volume or by power. The COE is calculated from the following equation [12,37]:

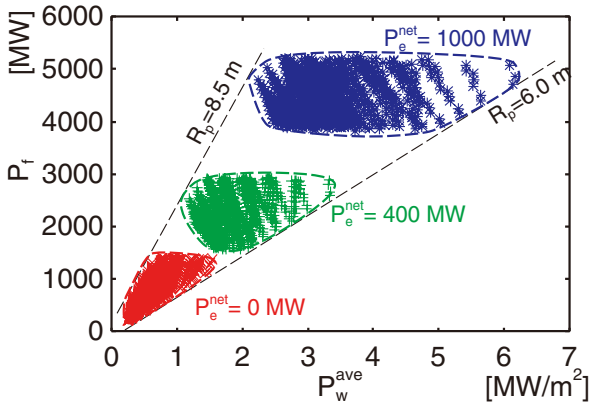

Fig. 11 P_w^{ave} and P_f for each net electric power P_e^{net} under the same conditions as in Figs. 3. The upper band edge is for R_p = 6.0 m while the lower band edge is for R_p = 8.5 m.

$$\mathrm{COE} = \frac{C_{ac} + C_{om} + C_{src} + C_{fuel}}{P_e\, 8760 f_{ave}} + C_{dis} + C_{dec}. \qquad (8)$$

The annual capital cost C_{ac} is calculated by multiplying the direct cost and factors such as an indirect cost multiplier, a capitalization factor, and a fixed charge rate. The annual maintenance cost C_{om} is calculated as a fraction of the value of the direct capical cost. The annual fuel cost C_{fuel} is calculated as a value proportional to the plant availability. C_{dis} and C_{dec} represent the cost of disposal and the cost of decommission, respectively.

This cost analysis model is installed into the system analysis code FUSAC, and economic performance parameters (COE, construction cost, and so on), are also calculated in the database mentioned in subsection **2.4**. This database is also applied to the analysis of the economic break-even condition.

4.2 Economic break-even condition in a world energy scenario

The typical value of the economic break-even condition is considered as the break-even price for introduction of fusion energy into the long-term world energy scenario, as introduced in Sec. **1**. Considering future uncertainties, e.g. energy demand scenarios and capacity utilization ratio of options in energy/environment technologies, some of authors have advanced an analysis for the break-even price of fusion energy using a long-term world energy and environmental model (this model is used for IPCC post SRES activity [18]), and estimate that the break-even price of the fusion energy for introduction in the year 2050 under the constraint of 550 ppm CO_2 concentration (twice the level during the Industrial Revolution) is in the range from 65 mill/kWh to 135 mill/kWh as shown in Fig. 12 [17]. If the cost of electricity

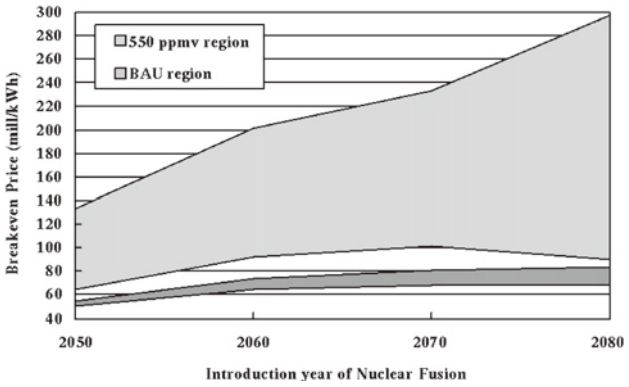

Fig. 12 Break-even price as a function of nuclear fusion introduction year for the CO_2-constraint case (550 ppmv) and the no-CO_2-constraint case (business-as-usual, BAU case) [17].

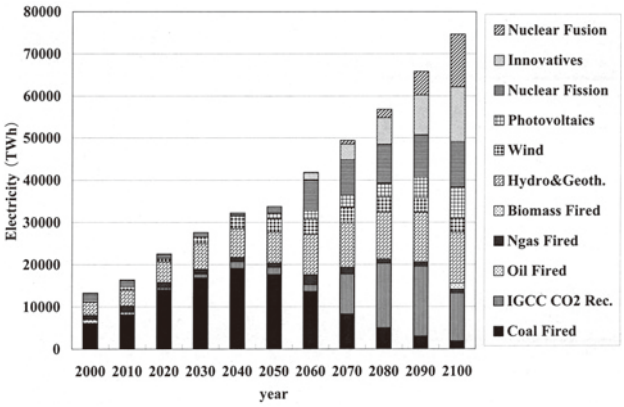

Fig. 13 Nuclear fusion's share of electricity assuming a 550 ppmv CO_2-concentration constraint. A break-even price of 65 mill/kWh is assumed for the nuclear fusion [17].

(COE) for fusion energy can achieve the lowest break-even price of this range, i.e. 65 mill/kWh in 2050, as a result of smooth introduction of the fusion energy, a 20% share of all produced electricity in 2100 can be expected to be supplied by fusion energy, as shown in Fig. 13. This range of the break-even price is estimated under plant availability of 60% for the first fusion power plant. This availability is low because unexpected outages of operation can be expected for the first fusion power plant. Of course, annual cost reduction of COE for 25 years after the first introduction is assumed because of improving plant availability, operation cost and so on.

Electricity by fusion energy in 2100 decreases with delay of the introduction year. For example, pushing back the introduction of fusion energy to 2070 will result in its having only about 4% share in 2100. The earlier the introduction of fusion energy, the more important the role in the long-term world energy scenario that fusion energy will play in 2100. The concentration of CO_2 in the atmosphere has been recognized as a critical environmental issue to date, and CO_2 emission has to be decreased by the year 2050, so as to keep the CO_2 level at 550 ppm (less than twice its level during the Industrial Revolution) by the year 2100 [18]. Fusion energy has the potential to reduce CO_2 emissions [38], and when its introduction in 2050 is realized, fusion energy can also contribute to keeping the CO_2 level in 2100 at 550 ppm or below. The key point for maximizing the role of fusion energy is how early fusion energy will be ready for electric power generation at a COE lower than the break-even price. Delayed introduction at a lower cost is not effective for maximizing the role of fusion energy. Hence, early demonstration of electric power generation on a plant scale is also important. That is why we chose the year 2050 as the target year for introducing fusion energy into the energy market.

4.3 Plasma performance required to achieve the economic break-even condition

The database constructed by FUSAC is also applied to this parametric analysis to clarify the plasma performance required to achieve a 2050 break-even price in the range of 65 mill/kWh to 135 mill/kWh. The result of the economic break-even condition for a tokamak fusion power plant with B_{tmax} = 16 T, P_e^{net} = 1000 MW and plant availability of 60% is shown in Fig. 14. Each operational space in Fig. 14 is composed

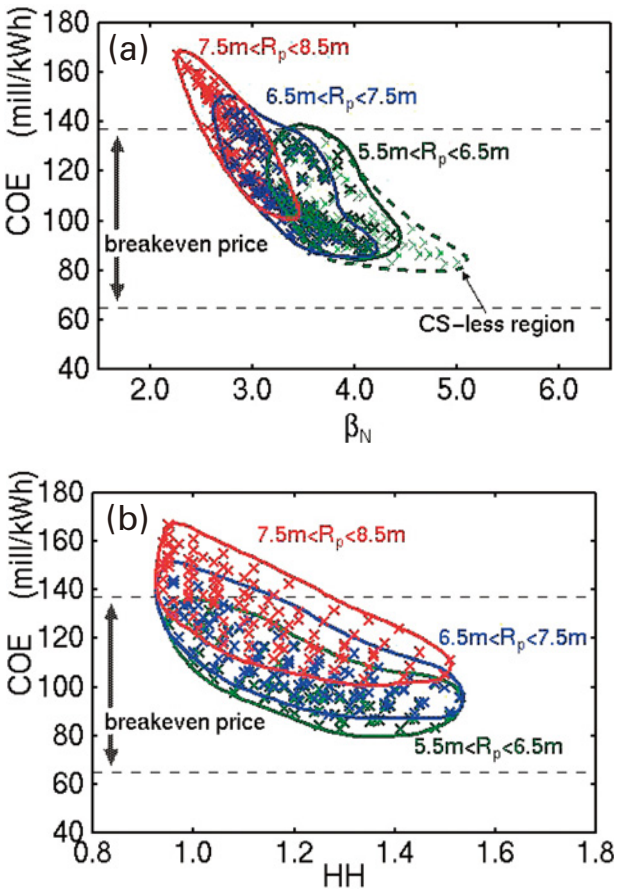

Fig. 14 (a) Normalized beta value β_N vs. COE for 16 T with the break-even price of fusion energy. The broken line shows the extension without CS coils (CS-less). (b) Confinement improvement factor *HH* vs. COE for 16 T with the break-even price of the fusion energy.

of the plots for possible operation points. Those operational points are calculated under the same conditions as in the previous section except: (1) thermal efficiency $\eta_e = 40\%$; and (2) the feasibility of a simplified radial build without CS coils (for which full non-inductive current ramp up is required). In the present study, when there is not sufficient space to locate the CS coils with the same B_{tmax} and coil current density J_{tfc} as the TF coil, the radial build is designed without CS coils.

Note that to achieve the most severe case of the break-even price 65 mill/kWh, $\beta_N > 5.0$ with smaller major radius $R_p < 6.0$ m is required. As shown in Fig. 14, a simplified radial build without a CS coil (CS-less region) is required to attain the lower boundary of COE with 5.5 m $< R_p <$ 6.5 m. This is because the current densities of TF and CS coils are not large enough to make sufficient space for a CS coil in the central torus region. In this result, the overall current density of the TF coil is $J_{tfc} \sim 10$ MA/m^2, which is almost the same as in the ITER design [27]. On the other hand, β_N more than 2.5 has the potential to achieve the upper region of the break-even price (~ 135 mill/kWh) in the long-term world energy scenario, while this β_N is not sufficient to guarantee the economic break-even condition. This β_N value is supposed to be attainable by the ITER advanced plasma performance aiming at steady-state operation [1], which implies that the completion of ITER advanced plasma with $\beta_N \sim 3.0$ may lead to the possibility of introducing the fusion energy in the world energy scenario.

Figure 14(b) shows the *HH* region required to achieve the break-even price. The higher the *HH*, the lower the COE because high *HH* reduces the cost for the current drive system. However, in contrast with β_N, the required *HH* region is almost the same through the range of 5.5 m $< R_p <$ 8.5 m. The most important suggestion in this figure is that there is no path with $HH < 0.9$ to introduction of the tokamak fusion reactor into the long-term world energy scenario. The fn_{GW} required to achieve the break-even price (not shown) has no clear dependence on COE. This is mainly because both the required density and the density are decreased as the major radius increases under the condition of almost the same fusion power P_f.

Figure 15 shows the dependence of B_{tmax} on COE in case of 5.5 m $< R_p <$ 6.5 m. These data reveal that an increase of B_{tmax} is very effective for a decrease of the required β_N under the condition of including a CS-less radial build. On the other hand, increasing B_{tmax} increases the lowest limit of COE under the condition of the same critical current density: Due to the increase of the coil volume or device size, the lower limit of the COE range of 19 T increases up to 90 mill/kWh. To get the merit of a high magnetic field, the current density of the superconducting coils also has to be improved. When TF coil current density of about 20 MA/m^2 is feasible at the same cost as a 10 MA/m^2 coil, the merit of the high magnetic field is clearly obtained; that is, the decrease of required β_N with the same COE as 13 T is possible, as shown in Fig. 15. For example, use of a high-temperature super conductor at a low temperature is effective at increasing the current density of

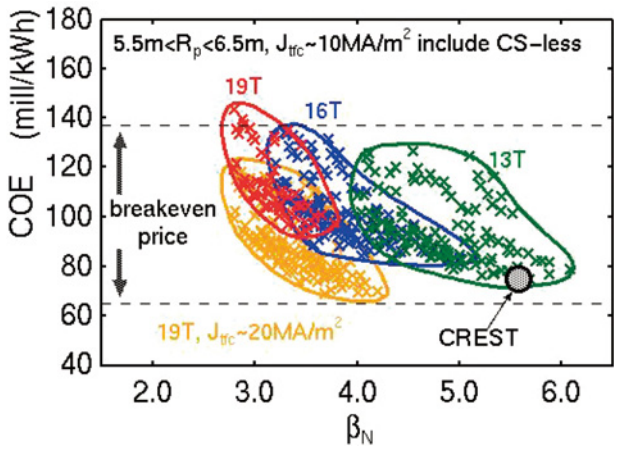

Fig. 15 Dependence of B_{tmax} on COE for 5.5 m $\le R_p \le$ 6.5 m and $J_{tfc} \sim 10$ MW/m^2 of TF and CS coils. The COE region for 19 T with $J_{tfc} \sim 20$ MW/m^2 is also shown. The CREST design point is located in the lower limit of the 13 T case.

TF coils. When advanced plasma with $\beta_N \sim 5.0$ is possible, a super conductor of 13 T is almost sufficient to achieve the lower region of the break-even price (65 mill/kWh). The design for the commercial plant CREST [33], where $R_p = 5.4$ m, $\eta_e = 41\%$, $B_{tmax} = 13$ T, is near the break-even price of 65 mill/kWh.

5. Summary

Forthcoming break-even conditions of tokamak plasma performance in fusion energy development are analyzed. In this analysis, an aspect ratio of $3.0 \le A \le 4.0$ (i.e., the conventional tokamak configuration) is used. We consider 2050 the target year for introducing fusion energy, and we clarify the following conditions: (1) the electric break-even condition required for fusion energy to be recognized as a suitable candidate for an alternative energy source, and (2) the economic break-even condition required for fusion energy to be selected as an alternative energy source in the world energy scenario. The electric break-even condition requires the simultaneous achievement of $1.2 < \beta_N < 2.7$, $0.8 < HH$, and $0.3 < fn_{GW} <$ 1.1 under the condition of $B_{tmax} = 16$ T, $\eta_e = 30\%$, and $P_{NBI} <$ 200 MW. It should be noted that the relatively moderate conditions of $\beta_N \sim 1.8$, $HH \sim 1.0$, and $fn_{GW} \sim 0.9$, which correspond to the ITER reference operation parameters, have a strong potential to achieve the electric break-even condition. The economic break-even condition requires $\beta_N \sim 5.0$ for the lower break-even price (65 mill/kWh) case under the conditions of $B_{tmax} = 16$ T, $\eta_e = 40\%$, plant availability 60%, and feasibility of a simplified radial build without a CS coil. The demonstration of steady-state operation with $\beta_N \sim 3.0$ in the ITER project leads to achievement of the upper region of break-even price in the world energy scenario. This implies that it is necessary to improve the plasma performance beyond the ITER advanced plasma operation in order to achieve the lower break-even price. This β_N requirement will be somewhat mitigated with higher B_{tmax}; however, the current densities of

TF and CS coils have to be simultaneously improved to obtain the clear merit of a higher magnetic field.

Acknowledgement

The authors would like to thank Drs. Y. Shimomura, N. Inoue, A. Kitsunezaki, S. Nishio, K. Tobita of the Japan Atomic Energy Agency for fruitful discussion. The authors are also grateful to Dr. Z. Yoshida of Univ. of Tokyo for his suggestion to write this paper. The authors also thank Drs. K. Tomabechi and T. Yoshida of CRIEPI for their thoughtful advice and encouragement.

References

[1] Technical basis for the ITER final design report *ITER EDA Documentation Series No.24* (Vienna: IAEA).
[2] Y. Asaoka *et al.*, Research and Development Steps for Commercial Use of Fusion Power Plants, CRIEPI Research Report T97077, Central Reseach Institute of Electric Power Industry, Tokyo, 1997 (In Japanese).
[3] R. Hiwatari *et al.*, Nucl. Fusion **44**, 106 (2004).
[4] European Commission Community Research *ITER, THE ROAD TO FUSION ENERGY* (Office for Official Publications of the European Communities, L-2985 Luxembourg) http://europa.eu.int/comm/research/energy/pdf/fusiontheroadn2.pdf.
[5] H. Bolt, Fast Track Concept in the European Fusion Program *Report of International Symposium for ITER (Tokyo, 24 January 2002)* http://www.naka.jaeri.go.jp/keijiban/iter-symposium/report.html (JAERI, Tokyo, 2002).
[6] M. Kikuchi *et al.*, Nucl. Fusion **30**, 265 (1990).
[7] R. Hiwatari *et al.*, Nucl. Fusion **45**, 96 (2005).
[8] K. Tobita *et al.*, "Design Study of Fusion DEMO Plant at JAERI" S6-14-O02 *Proc. 7th International Symposium on Fusion Nuclear Technology (Tokyo, May 2005)*.
[9] JET TEAM, The new experimental phase of JET and prospects for future operation IAEA-CN-60/A1-3 *Proc. 18th IAEA Fusion Energy conf. (Seville, September 1994)* (Vienna: IAEA).
[10] S. Ishida and JT-60 Team, Nucl. Fusion **39**, 1211 (1999).
[11] J. Sheffield *et al.*, Fusion Technology **9**, 1986 (1986).
[12] T. Yoshida *et al.*, Development of Cost Assessment Code of Fusion Power Reactors, CRIEPI Research Report T94001, Central Reseach Institute of Electric Power Industry, Tokyo, 1994 (In Japanese).
[13] R.L. Miller, Fusion Eng. Des. **41**, 393 (1998).
[14] K. Okano *et al.*, Fusion Eng. Des. **51-52**, 1025 (2000).
[15] J.G. Delene *et al.*, Fusion Technol. **39**, 228 (2001).
[16] K. Tokimatsu *et al.*, Nucl. Fusion **42**, 1289 (2002).
[17] K. Tokimatsu *et al.*, Energy Policy **31**, 775 (2003).
[18] Contribution of Working Group III to the Third Assessment Report of the Intergovernmental Panel on Climate Change, CLIMATE CHANGE 2001 Mitigation (UK: Cambridge University Press), 2001.
[19] R. Hiwatari *et al.*, J. Plasma Fusion Res. **78**, 991 (2002).
[20] T. Yoshida *et al.*, Development of Cost Assessment Code of Fusion Power Reactors *CRIEPI report No. T94001* (Central Research Institute of Electric Power Industry, Tokyo), 1994 (In Japanese).
[21] N. Uckan and ITER Physics Group ITER Physics Design Guidelines: 1989 *ITER Documentation Series No.10* (Vienna: IAEA), 1990.
[22] T. Mizoguchi *et al.*, Development of tokamak reactor conceptual design code "TRESCODE" —Conceptual design study of FY86 FER— JAERI-M 87-120 (Nakamachi: Naka Fusion Research Establishment, JAERI), 1987.
[23] F. Troyon *et al.*, Plasma Phys. Controlled Fusion **26**, 209 (1984).
[24] D. Mikkelsen and C. Singer, Nucl. Technol. Fusion **4**, 237 (1983).
[25] L. El-Guebaly *et al.*, Fusion Eng. Des. **38**, 139 (1997).
[26] Y. Murakami *et al.*, J. Plasma Fusion Res. **77**, 712 (2001).
[27] Technical basis for the ITER final design report (FDR) *ITER EDA Documentation Series No.16* (Vienna: IAEA) 1999.
[28] Y.R. Lin-Lin and R.D. Stambaugh, Nucl. Fusion **44**, 548 (2004).
[29] Y. Takahashi *et al.*, IEEE Trans. Appl. Superconduct., **12**, 1799 (2002).
[30] M. Seki *et al.*, Fusion Science and Technology **42**, 50 (2002).
[31] ITER Physics Expert Groups on Confinement and Transport and Confinement Modeling and Database, ITER Physics Basis Editors, Nucl. Fusion **39**, 2175 (1999).
[32] M. Greenwald *et al.*, Nucl. Fusion **28**, 2199 (1988).
[33] K. Okano *et al.*, Nucl. Fusion **40**, 63 (2000).
[34] F. Najmabadi *et al.*, ARIES-AT: An advanced tokamak, advanced technology fusion power plant steady-state tokamak reactor IAEA-CN-77/FTP2/15 *Proc. 18th IAEA Fusion Energy conf. (Sorrento, October 2000)* (Vienna: IAEA)
[35] S. Nishio *et al.*, J.Plasma Fusion Res. **78**, 1218 (2000).
[36] Y. Takase *et al.*, J. Plasma Fusion Res. **78**, 719 (2002).
[37] K. Tokimatsu *et al.*, Nucl. Fusion **38**, 885 (1998).
[38] M.I. Hoffert *et al.*, Science **298**, 981 (2002).